ACS Medicinal Chemistry Letters

Letter

pubs.acs.org/acsmedchemlett

FGFR1 Kinase Inhibitors: Close Regioisomers Adopt Divergent Binding Modes and Display Distinct Biophysical Signatures

Tobias Klein,* Julie Tucker,† Geoffrey A. Holdgate, Richard A. Norman, and Alexander L. Breeze*

Discovery Sciences, AstraZeneca R&D, Alderley Park, Macclesfield, Cheshire, SK10 4TG, U.K.

Supporting Information

ABSTRACT: The binding of a ligand to its target protein is often accompanied by conformational changes of both the protein and the ligand. This is of particular interest, since structural rearrangements of the macromolecular target and the ligand influence the free energy change upon complex formation. In this study, we use X-ray crystallography, isothermal titration calorimetry, and surface-plasmon resonance biosensor analysis to investigate the binding of pyrazolylaminopyrimidine inhibitors to FGFR1 tyrosine kinase, an important anticancer target. Our results highlight that structurally close analogs of this inhibitor series interact with FGFR1 with different binding modes, which are a consequence of conformational changes in both the protein and the ligand as well as the bound water network. Together with the collected kinetic and thermodynamic data, we use the protein−ligand crystal structure information to rationalize the observed inhibitory potencies on a molecular level.

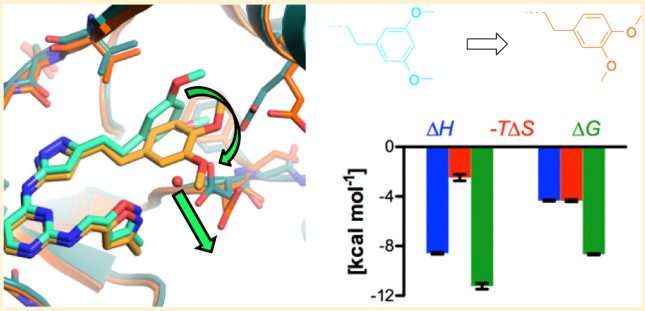

KEYWORDS: *Receptor tyrosine kinase, induced fit, protein−ligand interactions, X-ray crystallography, isothermal titration calorimetry, surface plasmon resonance*

Members of the fibroblast growth factor receptor (FGFR) family (FGFR1 to 4) serve as high affinity receptors for the fibroblast growth factors (FGFs)[1] and are key mediators of both developmental and disease-associated angiogenesis.[2] They are heavily implicated in the pathogenesis of tumor vascularization in a number of different tumor types, including breast,[3] pancreatic,[4] prostate,[5] and ovarian[6] carcinomas. Hence, they have been seen as attractive targets for the development of therapeutic agents[7] aimed at inhibiting tumor growth and metastasis through blockade of neovascularization. Recently, Norman et al. reported on the discovery of pyrazolylaminopyrimidines as potent FGFR1 inhibitors and their structure-based optimization that led to the identification of compound **1** (Figure 1).[8] In our continuing studies aimed at optimizing ligand-binding site interactions, the substitution pattern of the 3,5-dimethoxyphenyl group of **1** was varied. Interestingly, a tight structure−activity relationship was observed: moving one methoxy function from the 5- to the 4-position (compound **2**) resulted in a drop of inhibitory potency/binding affinity of almost 2 orders of magnitude (Figure 1). Intrigued by this finding, we set about investigating the interaction between FGFR1 kinase and the selected pyrazolylaminopyrimidine inhibitors **1**−**3** using structural and biophysical analysis. Comparisons of the inhibitor binding modes as well as the accompanying kinetic and thermodynamic signatures provide detailed insights into the molecular determinants governing the different affinities of these structurally close inhibitors toward FGFR1 kinase.

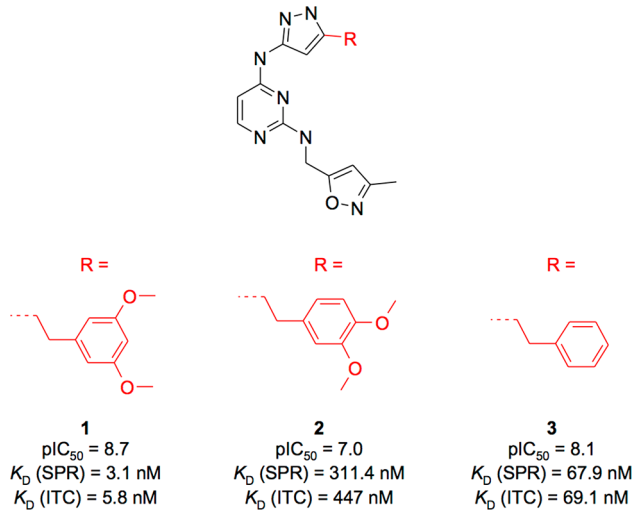

Figure 1. Structure, inhibitory potency, and binding affinity of pyrazolylaminopyrimidine-based inhibitors. Potency data presented as pIC_{50} ($pIC_{50} = -\log_{10}(IC_{50})$).

The crystal structure of FGFR1 in complex with **1** revealed the inhibitor to bind as expected with the pyrazolylaminopyr-

Received: October 19, 2013
Accepted: December 6, 2013
Published: December 6, 2013

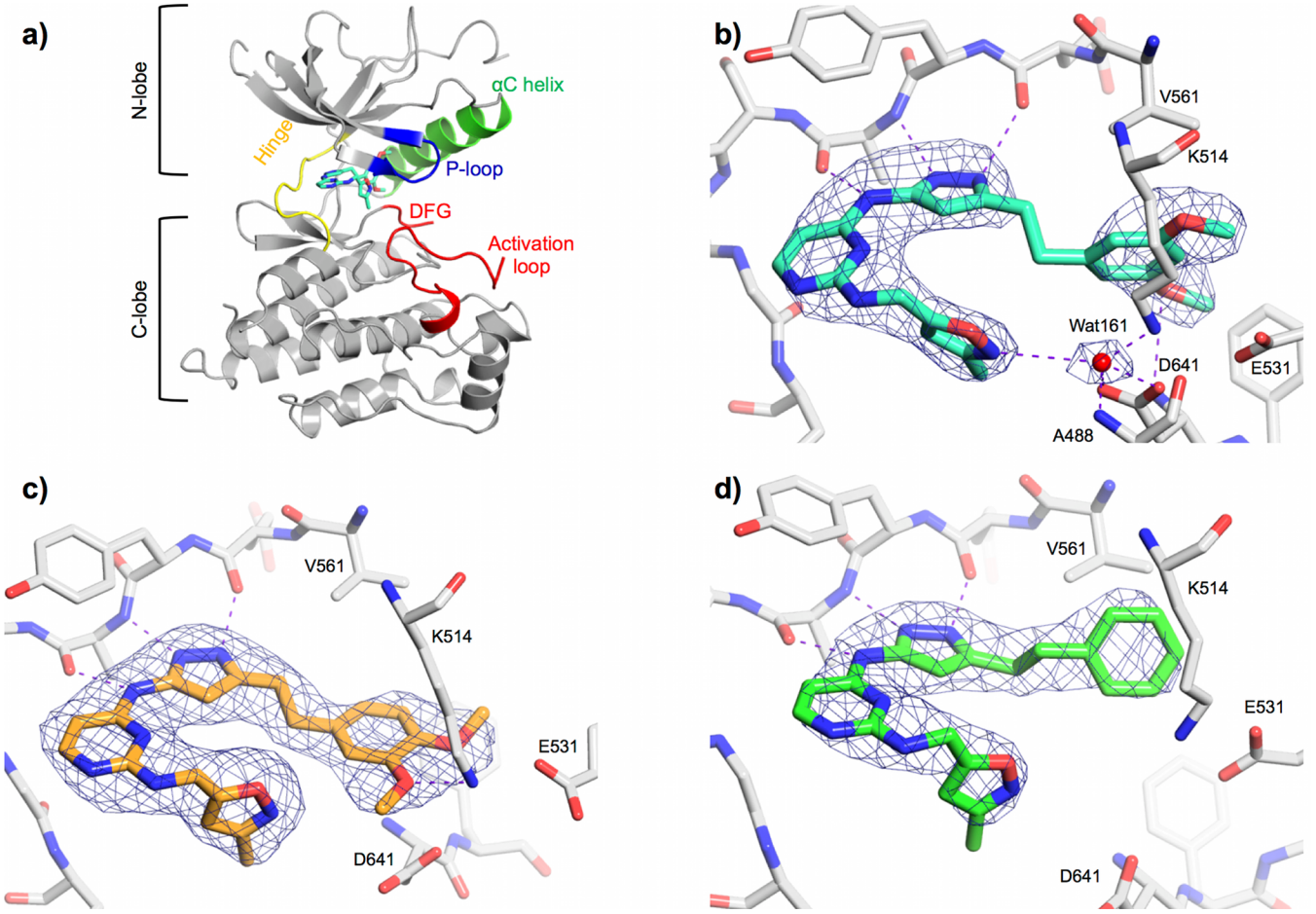

Figure 2. Crystal structures reveal differential inhibitor binding modes. (a) The overall structure of FGFR1 in complex with inhibitor **1** (cyan) exhibits a classical two-lobed kinase fold. The hinge region (yellow), P-loop (blue), activation loop (red), and C helix (green) are highlighted. (b) FGFR1 kinase in complex with **1** as determined at 2.57 Å resolution. (c) FGFR1 kinase in complex with **2** as determined at 2.19 Å resolution. (d) FGFR1 kinase in complex with **3** as determined at 2.50 Å resolution. The electron densities of compounds **1**, **2**, and **3** and Wat161 are represented as blue meshes calculated as $F_o - F_c$ OMIT maps contoured at 3.0σ. Polar interactions are indicated as dotted lines, and bound water molecules are shown as red spheres.

imidine core, forming three hydrogen bonds to the hinge region of the kinase domain. The methyl isoxazole protrudes into a constricted indentation at the base of the ATP pocket, which was previously referred to as the "pit" region,[8] and the nitrogen of this heterocycle makes a further hydrogen bond to a water molecule (Wat161 in chain A and Wat163 in chain B, respectively). This water molecule in turn is hydrogen-bonded to the side chains of protein kinase-conserved Lys514 and Asp641 and the backbone nitrogen of Ala488 (Figure 2b). Thus, this water molecule is in a binding site that provides the maximum number of hydrogen-bonding partners, suggesting that the enthalpic gain resulting from the formation of hydrogen bonds likely compensates the entropic penalty incurred by restriction of rotational and translational degrees of freedom through sequestration from bulk water.[9]

Interestingly, a water molecule in a closely equivalent location occurs in six further FGFR1−ligand complexes (PDB codes: 2FGI,[10] 3TTO,[11] 3C4F,[12] 3GQL,[13] 3RHX,[14] and 1AGW)[15] and also in ligand-bound complexes of other kinases such as ABL (PDB code: 2GQG,[16] 1OPJ),[17] SRC (PDB code: 1Y57),[18] or JAK1 (PDB code: 4E5W;[19] Supporting Information Figure S1). In some of the structures, the conserved water molecule mediates a hydrogen bond to the ligand, as observed for the FGFR1−**1** complex; furthermore, it interconnects different structural features of the kinase domain (P-loop, A-loop, αC helix, β3 sheet) through hydrogen bonds. Thus, a water molecule in this position seems to contribute to the overall stability of the complex.[20]

As shown in Figure 2b, the dimethoxy phenyl group of **1** binds to the hydrophobic pocket, where it packs against the gatekeeper residue Val561. One of the methoxy groups makes a hydrogen bond with the amide nitrogen of Asp641, part of the protein kinase-conserved Asp-Phe-Gly triad at the beginning of the activation loop. Hence, the 3,5-dimethoxyphenyl group of **1** shows the same interactions with FGFR1 as reported for the dimethoxy substituted phenyl ring of the potent pyridopyrimidine inhibitor PD173074 (Supporting Information Figure S2). In this inhibitor class the 3,5-dimethoxyphenyl motif was identified as a key selectivity determinant that is uniquely tolerated by FGFR. Changing the substitution pattern of the phenyl ring from 3,5-dimethoxy (IC_{50} = 60 nM) to 3,4-dimethoxy (IC_{50} = 20 μM) also resulted in a dramatic loss of inhibitory potency.[21] The molecular origin of this significant difference in potency, however, has, to date, remained elusive.

The crystal structure of the FGFR1−**2** complex provides insights in this regard. It shows that replacement of the 3,5-dimethoxyphenyl group in **1** by a 3,4-dimethoxyphenyl moiety (compound **2**) significantly changes the FGFR1-bound

dx.doi.org/10.1021/ml4004205 | ACS Med. Chem. Lett. 2014, 5, 166−171

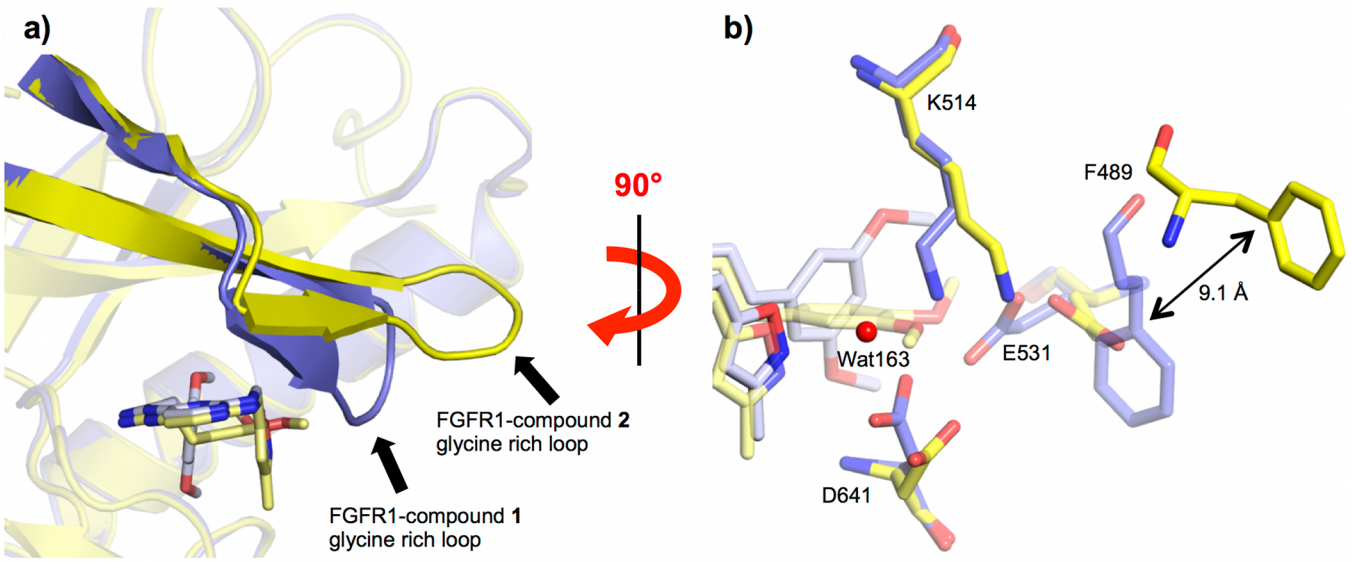

Figure 3. Inhibitor-induced conformational changes. (a) Overlaid protein conformations of FGFR1 in complex with **1** (blue cartoon representation) and FGFR1 in complex with **2** (yellow cartoon representation). (b) Detail of the conformational change induced by the binding of **2** in FGFR1 (yellow stick representation), relative to FGFR1 in complex with inhibitor **1** (blue stick representation); bound water molecules are shown as red spheres.

inhibitor conformation (Figure 2c). In contrast to **1** and PD173074, which bind to FGFR1 with the planes of the phenyl ring approximately perpendicular to the plane of the pyrazolylaminopyrimidine and pyrido[2,3-d]pyrimidine rings (Figure 2b; Supporting Information Figure S2), the 3,4-dimethoxy substitution in **2** forces the phenyl and the pyrazolylaminopyrimidine rings into a parallel geometry, most likely for steric reasons (Figure 2c).

A regiospecific effect of phenyl substitutions on ligand potency has previously been discussed by Hajduk et al. In their statistical analysis of common chemical substitutions on ligand potency, they observed that the frequencies of achieving 10-fold losses in potency for dimethoxy substitutions are 2-fold higher for the 3,4- than for the 3,5-substitution pattern.[22]

The FGFR1-bound conformation of the desmethoxy analog **3** (Figure 2d) is similar to the previous conformation of a close analog having a bromine substituent on the pyrimidine ring in complex with FGFR1 (PDB code: 4F65).[8] In contrast to the structures of FGFR1 in complex with the bromine substituted analog or **1**, respectively, the observed electron density did not support the presence of a water molecule at the FGFR1−**3** interface. In this structure the plane of the phenyl ring is also perpendicular to the plane of the core. An alternative conformation of the ethyl linker between the pyrazole and the phenyl rings of **3**, however, positions the phenyl group of **3** close to the hydrophobic side chains of Val491, Val561, and Val559. In contrast, in the FGFR1−**1** complex, the dimethoxy phenyl group is shifted toward the beginning of the activation loop. This facilitates the formation of the hydrogen bond with the amide nitrogen of Asp641 and avoids steric clashes with the N-terminal part of the ATP binding cleft (structure of the protein kinase catalytic domain reviewed in Schwartz and Murray[23]).

Compared with the FGFR1−**1** complex, binding of **2** favored a different conformation of the glycine rich nucleotide-binding loop (P-loop; Figure 3). In the structure of FGFR1 in complex with **1**, the P-loop adopts a conformation that packs tightly against the inhibitor, with Phe489 capping the hydrophobic pocket in which the dimethoxy phenyl group binds. A similar P-loop conformation that shields the ligand from the surrounding solvent has been observed for p38α kinase in complex with the inhibitor Scios-469 (PDB code: 3HUB).[24] In contrast, the P-loop adopts a less ordered conformation in the FGFR1−**2** structure and does not closely pack against the inhibitor (Figure 3a). Most likely, this is due to the altered conformation of the 3,4-dimethoxy-substituted phenyl group, which does not allow **2** to enter as deeply into the hydrophobic pocket as **1**. On the other hand, this causes the side chains of Lys514, Glu531, and Asp641 to adopt alternative conformations, which allow accommodation of the 3,4-dimethoxy phenyl substituent of **2** but would clash with the P-loop conformation observed in the FGFR1−**1** structure (Figure 3b). The solvent-exposed 3-methoxy group of **2** makes a polar contact to the side chain of Lys514, but the hydrogen bond to the amide nitrogen of Asp641 is lost. We hypothesize that ligand-induced conformational changes in the glycine-rich loop contribute substantially to the affinity differences between inhibitors **1** and **2**, corroborating the previously stated importance of the P-loop as determinant for inhibitor selectivity and affinity.[24] Thus, the design of kinase inhibitors that interact directly with the P-loop could provide a route to inhibitors with optimized selectivity and affinity profiles.

The different positioning of the 3-methoxy group of **2** also results in the displacement of the optimally coordinated, conserved water molecule from its binding site. Since this water molecule mediates a hydrogen bond between FGFR1 and **1** as well as interconnecting the P-loop, the A-loop, and the β3 sheet by interactions with Ala488, Asp641, and Lys514, respectively, its absence in the FGFR1−**2** complex might also be a determinant for the reduced complex stability.

To evaluate whether the observed structural differences translate directly into thermodynamic and kinetic effects, we have analyzed the thermodynamic and kinetic profiles of the FGFR1−inhibitor interactions. Changes in the thermodynamic parameters for binding across inhibitors **1**−**3** were determined by isothermal titration calorimetry (ITC). As shown in Figure

dx.doi.org/10.1021/ml4004205 | *ACS Med. Chem. Lett.* 2014, 5, 166−171

4, the binding free energy of **1** (ΔG = −11.2 kcal mol^{-1}) is clearly dominated by an enthalpic component (ΔH = −8.6 kcal mol^{-1}). Replacement of the 3,5-dimethoxyphenyl group in **1** by a 3,4-dimethoxyphenyl substituent (compound **2**) is accompanied by a remarkable relative loss in enthalpy ($\Delta\Delta H_{1\rightarrow2}$ = 4.3 kcal mol^{-1}). The observed changes in the polar FGFR1−inhibitor interactions, including the liberation of a hydrogen-bonded water molecule from its binding site, may contribute to this large loss, corroborating the hypothesis that this water molecule makes a favorable contribution to the binding free energy due to the enthalpic gain resulting from four hydrogen bonds. Conversely, release of a bound water molecule into the bulk solvent is entropically favorable: taken together with the more flexible P-loop conformation in the FGFR1−**2** complex, the displacement of the water molecule may underlie the more favorable entropic component ($-T\Delta\Delta S_{1\rightarrow2}$ = −1.9 kcal mol^{-1}) in the binding of **2** relative to **1**.

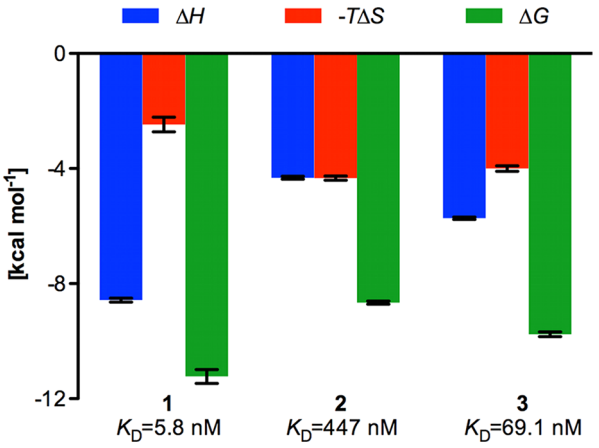

Figure 4. Thermodynamic parameters as determined by ITC. Data represent geometric means from at least two independent experiments; standard errors are shown as error bars (values and errors are presented in the Supporting Information).

The gain in entropy partly compensates the degradation in enthalpy, and therefore, inhibitor **2** binds with a balanced thermodynamic profile, where both the enthalpy and entropy terms contribute equally (at standard concentration) to the (reduced) binding affinity (ΔH = −4.3 kcal mol^{-1} and $-T\Delta S$ = −4.3 kcal mol^{-1}). Biela et al. have observed a comparable change in enthalpy and entropy for a series of thermolysin inhibitors where enlargement of an alkyl side chain of the inhibitors led to the displacement of a hydrogen-bonded water molecule at the interface with the bulk solvent.[25]

Our observation in FGFR1 illustrates that in some cases the enthalpy gain resulting from formation of additional hydrogen bonds more than offsets the entropic penalty that must be paid for immobilizing the water involved. Therefore, incorporating functional groups that are able to interact with water molecules mediating hydrogen bond bridges to the protein might be generally beneficial for ligand affinity. A corollary is that strategies involving expulsion of such structural waters may in many cases be deleterious to affinity.

Omitting the methoxy groups on the phenyl ring (compound **3**) increases the binding free energy relative to **2** ($\Delta\Delta G_{2\rightarrow3}$ = −1.1 kcal mol^{-1}) by approximately 1 order of magnitude whereas it decreases it relative to **1** ($\Delta\Delta G_{1\rightarrow3}$ = 1.5 kcal mol^{-1}) by a similar margin.

Binding kinetic data for the selected pyrazolylaminopyrimidines were obtained using surface plasmon resonance (SPR) biosensor analysis (Figure 5) and demonstrated binding affinities similar to those measured by ITC. The kinetic analysis highlights the fact that, despite similar association rate constants, the dissociation rates of inhibitors **1**−**3** vary considerably and are the key driver for the observed differences in the overall binding affinity. The dissociation rate of **1** (k_{off} = 1.1 × 10^{-2} s^{-1}) is 23-fold slower than that seen for **3** (k_{off} = 2.5 × 10^{-1} s^{-1}) and as much as 46-fold slower than that observed for **2** (k_{off} = 5.1 × 10^{-1} s^{-1}; Figure 5).

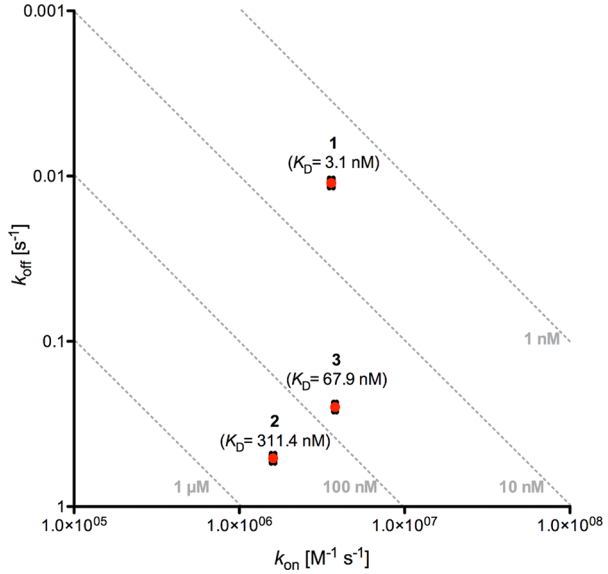

Figure 5. Kinetic value plot of association rate constant (k_{on}) versus dissociation rate constant (k_{off}). The affinities (K_D) were calculated from the equation $K_D = k_{off}/k_{on}$; broken lines represent affinity isotherms. Data represent geometric means from at least two independent experiments; standard errors are shown as error bars (values and errors are presented in the Supporting Information).

Relating the biophysical signatures to the structural binding modes, a trend becomes apparent: a parallel orientation of the plane of the phenyl ring relative to the plane of the pyrazolylaminopyrimidine core of the ligand (compound **2**) leading to the displacement of a conserved water molecule is characterized by a less favorable enthalpic contribution to the binding free energy and a faster dissociation rate than orthogonal geometries (compounds **1** and **3**). Comparing **3** and **1** shows that anchoring of the perpendicular ring conformation by introduction of substituents that make additional interactions further increases the enthalpic contribution to the binding energy and decreases the dissociation rate constant.

In conclusion, we have performed a comprehensive study of the binding of pyrazolylaminopyrimidine inhibitors to FGFR1 tyrosine kinase. The striking differences observed between inhibitor binding modes highlight the fact that minor changes in the substitution pattern of the ligand (**1** (3,5-dimethoxyphenyl) versus **2** (3,4-diemthoxyphenyl)) can have a profound effect on the enzyme-bound conformation. Inhibitor **1** binds to FGFR1 with the plane of the phenyl ring in a perpendicular orientation to the plane of the pyrazolylaminopyrimidine core, whereas in the FGFR1−**2** complex these two planes are aligned parallel to one another. A corollary of the altered geometry is

dx.doi.org/10.1021/ml4004205 | ACS Med. Chem. Lett. 2014, 5, 166−171

release of an evidently enthalpically favorable bound water molecule, coupled with reduced ordering of the P-loop. The complex with **2** is characterized by a smaller enthalpic contribution to the binding free energy and a significantly faster dissociation rate constant than that of the FGFR1−**1** complex, resulting in the observed potency differences. Further studies are currently underway in our laboratory using NMR to understand the contribution of protein dynamics to the observed global biophysical signatures of these and other FGFR1 inhibitors. Taken together with the data reported here, these insights will inform design strategies for improved drug candidates targeting FGFR1 kinase.

■ ASSOCIATED CONTENT

Supporting Information

Experimental details for biophysical assays and X-ray structure determination; Supplementary Figures S1−S3; Supplementary Tables S1−S3. This material is available free of charge via the Internet at http://pubs.acs.org.

Accession Codes

Coordinates and structure factors have been deposited in the Protein Data Bank with the following accession numbers: FGFR1−**1** complex, 4NK9; FGFR1−**2** complex, 4NKA; FGFR1−**3** complex, 4NKS.

■ AUTHOR INFORMATION

Corresponding Authors

*T.K.: E-mail, tobias.klein@astrazeneca.com; phone, +44 1625 512692.

*A.L.B.: E-mail, alex.breeze@astrazeneca.com; phone: +44 1625 514651.

Present Address

†J.T.: Northern Institute for Cancer Research, Paul O'Gorman Building, Medical School, Newcastle University, Framlington Place, Newcastle upon Tyne, NE2 4HH, U.K.

Author Contributions

T.K., G.A.H., R.A.N., and A.L.B. designed research; T.K., J.T., and R.A.N. performed research; T.K., J.T., G.A.H., R.A.N., and A.L.B. analyzed data; and all authors wrote the paper. All authors have given approval to the final version of the manuscript.

Notes

This work was funded as part of the AstraZeneca Internal Post Doctoral program. All the authors are employees (and stockholders) of AstraZeneca UK Ltd. or were at the time that this study was conducted.

■ ACKNOWLEDGMENTS

The authors thank J. Griesbach and H.K. Pollard for their assistance in protein purification and the "AZ FGFR chemistry team" for the synthesis of compounds **1**−**3**.

■ ABBREVIATIONS

FGF, fibroblast growth factor; FGFR, fibroblast growth factor receptor; FGFR1, fibroblast growth factor receptor 1; SPR, surface plasmon resonance; ITC, isothermal titration calorimetry; NMR, nuclear magnetic resonance

■ REFERENCES

(1) Eswarakumar, V. P.; Lax, I.; Schlessinger, J. Cellular signaling by fibroblast growth factor receptors. *Cytokine Growth Factor Rev.* **2005**, *16*, 139−149.

(2) Turner, N.; Grose, R. Fibroblast growth factor signalling: from development to cancer. *Nat. Rev. Cancer* **2010**, *10*, 116−29.

(3) Koziczak, M.; Holbro, T.; Hynes, N. E. Blocking of FGFR signaling inhibits breast cancer cell proliferation through down-regulation of D-type cyclins. *Oncogene* **2004**, *23*, 3501−8.

(4) Chen, G.; Tian, X.; Liu, Z.; Zhou, S.; Schmidt, B.; Henne-Bruns, D.; Bachem, M.; Kornmann, M. Inhibition of endogenous SPARC enhances pancreatic cancer cell growth: modulation by FGFR1-III isoform expression. *Br. J. Cancer* **2010**, *102*, 188−95.

(5) Feng, S.; Shao, L.; Yu, W.; Gavine, P.; Ittmann, M. Targeting fibroblast growth factor receptor signaling inhibits prostate cancer progression. *Clin. Cancer Res.* **2012**, *18*, 3880−8.

(6) Zhang, Y.; Guo, K. J.; Shang, H.; Wang, Y. J.; Sun, L. G. Expression of aFGF, bFGF, and FGFR1 in ovarian epithelial neoplasm. *Chin. Med. J. (Engl.)* **2004**, *117*, 601−3.

(7) Katoh, M.; Nakagama, H. FGF Receptors: Cancer Biology and Therapeutics. *Med. Res. Rev.* **2013**, DOI: 10.1002/med.21288.

(8) Norman, R. A.; Schott, A.-K.; Andrews, D. M.; Breed, J.; Foote, K. M.; Garner, A. P.; Ogg, D.; Orme, J. P.; Pink, J. H.; Roberts, K.; Rudge, D. A.; Thomas, A. P.; Leach, A. G. Protein-ligand crystal structures can guide the design of selective inhibitors of the FGFR tyrosine kinase. *J. Med. Chem.* **2012**, *55*, 5003−12.

(9) Ladbury, J. E. Just add water! The effect of water on the specificity of protein-ligand binding sites and its potential application to drug design. *Chem. Biol.* **1996**, *3*, 973−980.

(10) Mohammadi, M.; Froum, S.; Hamby, J. M.; Schroeder, M. C.; Panek, R. L.; Lu, G. H.; Eliseenkova, A. V.; Green, D.; Schlessinger, J.; Hubbard, S. R. Crystal structure of an angiogenesis inhibitor bound to the FGF receptor tyrosine kinase domain. *EMBO J.* **1998**, *17*, 5896−904.

(11) Guagnano, V.; Furet, P.; Spanka, C.; Bordas, V.; Le Douget, M.; Stamm, C.; Brueggen, J.; Jensen, M. R.; Schnell, C.; Schmid, H.; Wartmann, M.; Berghausen, J.; Drueckes, P.; Zimmerlin, A.; Bussiere, D.; Murray, J.; Graus Porta, D. Discovery of 3-(2,6-Dichloro-3,5-dimethoxy-phenyl)-1-{6-[4-(4-ethyl-piperazin-1-yl)-phenylamino]-pyrimidin-4-yl}-1-methyl-urea (NVP-BGJ398), A Potent and Selective Inhibitor of the Fibroblast Growth Factor Receptor Family of Receptor Tyrosine Kinase. *J. Med. Chem.* **2011**, *54*, 7066−7083.

(12) Tsai, J.; Lee, J. T.; Wang, W.; Zhang, J.; Cho, H.; Mamo, S.; Bremer, R.; Gillette, S.; Kong, J.; Haass, N. K.; Sproesser, K.; Li, L.; Smalley, K. S. M.; Fong, D.; Zhu, Y.-L.; Marimuthu, A.; Nguyen, H.; Lam, B.; Liu, J.; Cheung, I.; Rice, J.; Suzuki, Y.; Luu, C.; Settachatgul, C.; Shellooe, R.; Cantwell, J.; Kim, S.-H.; Schlessinger, J.; Zhang, K. Y. J.; West, B. L.; Powell, B.; Habets, G.; Zhang, C.; Ibrahim, P. N.; Hirth, P.; Artis, D. R.; Herlyn, M.; Bollag, G. Discovery of a selective inhibitor of oncogenic B-Raf kinase with potent antimelanoma activity. *Proc. Natl. Acad. Sci. U.S.A.* **2008**, *105*, 3041−3046.

(13) Bae, J. H.; Lew, E. D.; Yuzawa, S.; Tomé, F.; Lax, I.; Schlessinger, J. The Selectivity of Receptor Tyrosine Kinase Signaling Is Controlled by a Secondary SH2 Domain Binding Site. *Cell* **2009**, *138*, 514−524.

(14) Eathiraj, S.; Palma, R.; Hirschi, M.; Volckova, E.; Nakuci, E.; Castro, J.; Chen, C.-R.; Chan, T. C. K.; France, D. S.; Ashwell, M. A. A novel mode of protein kinase inhibition exploiting hydrophobic motifs of autoinhibited kinases: discovery of ATP-independent inhibitors of fibroblast growth factor receptor. *J. Biol. Chem.* **2011**, *286*, 20677−87.

(15) Mohammadi, M.; McMahon, G.; Sun, L.; Tang, C.; Hirth, P.; Yeh, B. K.; Hubbard, S. R.; Schlessinger, J. Structures of the Tyrosine Kinase Domain of Fibroblast Growth Factor Receptor in Complex with Inhibitors. *Science* **1997**, *276*, 955−960.

(16) Tokarski, J. S.; Newitt, J. A.; Chang, C. Y. J.; Cheng, J. D.; Wittekind, M.; Kiefer, S. E.; Kish, K.; Lee, F. Y. F.; Borzillerri, R.; Lombardo, L. J.; Xie, D.; Zhang, Y.; Klei, H. E. The structure of Dasatinib (BMS-354825) bound to activated ABL kinase domain elucidates its inhibitory activity against imatinib-resistant ABL mutants. *Cancer Res.* **2006**, *66*, 5790−7.

(17) Nagar, B.; Hantschel, O.; Young, M. A.; Scheffzek, K.; Veach, D.; Bornmann, W.; Clarkson, B.; Superti-Furga, G.; Kuriyan, J.

Structural Basis for the Autoinhibition of c-Abl Tyrosine Kinase. *Cell* **2003**, *112*, 859−871.
(18) Cowan-Jacob, S. W.; Fendrich, G.; Manley, P. W.; Jahnke, W.; Fabbro, D.; Liebetanz, J.; Meyer, T. The Crystal Structure of a c-Src Complex in an Active Conformation Suggests Possible Steps in c-Src Activation. *Structure* **2005**, *13*, 861−871.
(19) Kulagowski, J. J.; Blair, W.; Bull, R. J.; Chang, C.; Deshmukh, G.; Dyke, H. J.; Eigenbrot, C.; Ghilardi, N.; Gibbons, P.; Harrison, T. K.; Hewitt, P. R.; Liimatta, M.; Hurley, C. A.; Johnson, A.; Johnson, T.; Kenny, J. R.; Bir Kohli, P.; Maxey, R. J.; Mendonca, R.; Mortara, K.; Murray, J.; Narukulla, R.; Shia, S.; Steffek, M.; Ubhayakar, S.; Ultsch, M.; van Abbema, A.; Ward, S. I.; Waszkowycz, B.; Zak, M. Identification of Imidazo-Pyrrolopyridines as Novel and Potent JAK1 Inhibitors. *J. Med. Chem.* **2012**, *55*, 5901−5921.
(20) Levy, Y.; Onuchic, J. N. Water Mediation in Protein Folding and Molecular Recognition. *Annu. Rev. Biophys. Biomol. Struct.* **2006**, *35*, 389−415.
(21) Connolly, C. J. C.; Hamby, J. M.; Schroeder, M. C.; Barvian, M.; Lu, G. H.; Panek, R. L.; Amar, A.; Shen, C.; Kraker, A. J.; Fry, D. W.; Klohs, W. D.; Doherty, A. M. Discovery and structure-activity studies of a novel series of pyrido[2,3-d]pyrimidine tyrosine kinase inhibitors. *Bioorg. Med. Chem. Lett.* **1997**, *7*, 2415−2420.
(22) Hajduk, P. J.; Sauer, D. R. Statistical Analysis of the Effects of Common Chemical Substituents on Ligand Potency. *J. Med. Chem.* **2008**, *51*, 553−564.
(23) Schwartz, P. A.; Murray, B. W. Protein kinase biochemistry and drug discovery. *Bioorg. Chem.* **2011**, *39*, 192−210.
(24) Simard, J. R.; Getlik, M.; Grütter, C.; Schneider, R.; Wulfert, S.; Rauh, D. Fluorophore Labeling of the Glycine-Rich Loop as a Method of Identifying Inhibitors That Bind to Active and Inactive Kinase Conformations. *J. Am. Chem. Soc.* **2010**, *132*, 4152−4160.
(25) Biela, A.; Nasief, N. N.; Betz, M.; Heine, A.; Hangauer, D.; Klebe, G. Dissecting the Hydrophobic Effect on the Molecular Level: The Role of Water, Enthalpy, and Entropy in Ligand Binding to Thermolysin. *Angew. Chem., Int. Ed.* **2013**, *52*, 1822−1828.